Urania
Jurnal Ilmiah Daur Bahan Bakar Nuklir

Beranda jurnal: https://ejournal.brin.go.id/urania

THE EFFECT OF CURRENT DENSITY ON THE SURFACE MORPHOLOGY IN THE THIN COATING PROCESS OF NICKEL ON Zr-2 USING THE ELECTROPLATING METHOD

Yusuf Gigih Wicaksono[1,2], Ridwan[2], Azwar Manaf[1*]
[1]Department of Physics, Faculty of Mathematics and Natural Science, Universitas Indonesia
Depok, Jawa Barat 16424
[2]Research Center for Nuclear Material and Radioactive Waste Technology – BRIN
Kawasan Sains dan Teknologi B.J Habibie Gd. 720, Serpong, Tangerang Selatan, Banten 15314
e-mail: azwar@ui.ac.id

(Submitted: 19–02–2025, Revised: 11–06–2025, Accepted: 04–07–2025)

ABSTRACT

THE EFFECT OF CURRENT DENSITY ON THE SURFACE MORPHOLOGY IN THE THIN-COATING PROCESS OF NICKEL ON Zr-2 USING THE ELECTROPLATING METHOD. After the Fukushima-Daiichi reactor accident in 2011, one of the research and development focuses of nuclear fuel worldwide has been on coatings for Enhanced Accident Tolerant Fuels (EATF). Chromium (Cr) coatings are considered suitable due to their high oxidation resistance; however, Cr has limitations, particularly its poor diffusion on certain materials such as zirconium (Zr). Nickel coatings are therefore used as an interlayer to overcome the diffusion problem of chromium on zirconium substrates. Several surface coating methods are available, such as physical vapor deposition (PVD), chemical vapor deposition (CVD), high velocity oxygen fuel (HVOF), detonation gun (D-Gun), and electroplating. Electroplating was chosen in this study because of its high productivity, simple equipment, and low cost. The purpose of this research was to investigate the effect of current density on the surface morphology in the electroplating of Zr-2 with nickel. Electroplating is a process in which metal ions in an electrolyte solution are driven by an electric field to deposit onto a material. The electrolyte solution used in this study consisted of 200 g/L $NiSO_4 \cdot 6H_2O$ as the nickel source, 35 g/L $NiCl_2 \cdot 6H_2O$ as the activator, and 30 g/L H_3BO_3 as the pH buffer. The current densities applied were 0.015 A/cm², 0.025 A/cm², and 0.05 A/cm². After deposition, hardness tests were conducted, and the surface morphology was examined using SEM and EDS. The results showed that increasing the current density led to larger average nickel grain sizes, namely 4.68 µm, 6.19 µm, and 6.84 µm, as well as larger pore areas on the surface, namely 6.5 µm², 20.85 µm², and 27.98 µm². Micro-Vickers hardness tests indicated that higher current density increased hardness values, measured at 163.48 HV, 178 HV, and 234.25 HV, respectively. Cross-sectional SEM analysis revealed that the coating produced at a current density of 0.015 A/cm² showed better quality compared to higher current densities. This was evidenced by smaller pore areas, thinner coating thickness (7.44 µm compared to 19.17 µm and 8.42 µm), and the absence of defects at the coating–substrate interface, which were observed at 0.025 and 0.05 A/cm². To achieve thickness values closer to calculations, uniform spacing between the cathode and anode as well as the use of a fresh electrolyte solution are recommended. The use of a nickel interlayer can be a promising option to improve the surface performance of Zr-2.

Keywords: electroplating, nickel, zirconium-2, thin film, current density.

INTRODUCTION

Since the 1960s, zirconium-based alloys have been widely used as nuclear fuel cladding in light water reactors (LWRs), due to their low thermal neutron absorption cross-section, as well as their good oxidation resistance, neutron irradiation resistance, and ductility [1]. Following the Fukushima Daiichi reactor accident, one of the major focuses of nuclear fuel research and development worldwide has been coatings for Enhanced Accident Tolerant Fuels (EATF) [2][3]. In accident scenarios, such as the loss of coolant, the reactor core temperature can rise sharply, leading to oxidation of the zirconium cladding [4][5]. Once the fuel rod temperature reaches approximately 700 °C, the fuel may crack, exposing the interior of the zirconium alloy to the coolant environment, which in turn accelerates the temperature rise within the reactor [6].

Research on zirconium surface coatings has been carried out since the 1960s. At that time, the main objective was to improve the corrosion resistance of zirconium alloys oxidized by CO_2 during reactor operation, rather than to address loss-of-coolant accidents (LOCA) [7]. Chromium (Cr) coatings are considered suitable due to their high oxidation resistance; however, Cr also has a drawback, namely its poor diffusion capability on certain materials such as zirconium (Zr). To overcome this limitation, an intermediate material between Zr and Cr is required, with nickel (Ni) being one of the viable options [8][9]. The poor diffusion between Cr coatings and Zr substrates arises from differences in crystal structure, lattice parameters, and atomic radii. Cr has a body-centered cubic (BCC) structure with a lattice parameter of 2.8839 Å and an atomic radius of 0.1249 nm, whereas Zr has a hexagonal close-packed (HCP) structure with a lattice parameter of 3.2312 Å and an atomic radius of 0.1585 nm [10]. By first depositing a Ni layer onto the Zr substrate followed by heat treatment, the formation of Ni–Zr intermetallic phases can be promoted [9][11]. Meanwhile, the Cr layer can bond with the Ni layer through lattice matching.

Several coating techniques, including magnetron sputtering [12], plasma spraying [13,14], 3D laser cladding [15], arc ion plating [16], detonation gun (D-Gun), and vacuum arc plasma coating, present difficulties in depositing Zr uniformly on the inner surface of fuel cladding [10]. Electroplating was therefore selected in this study, as it offers high productivity, simple equipment requirements, and relatively low cost [5].

In the electroplating process, the sample is connected to the negative pole (cathode), while the coating material or another conductive material, such as platinum, is connected to the positive pole (anode), as illustrated in Figure 1 [16]. The deposition time required for the process was determined using Faraday's law. After the plating duration was established, Ni was deposited onto Zr-2 substrates through the electroplating method. The surface morphology of the resulting Ni coatings was subsequently characterized using a scanning electron microscope (SEM).

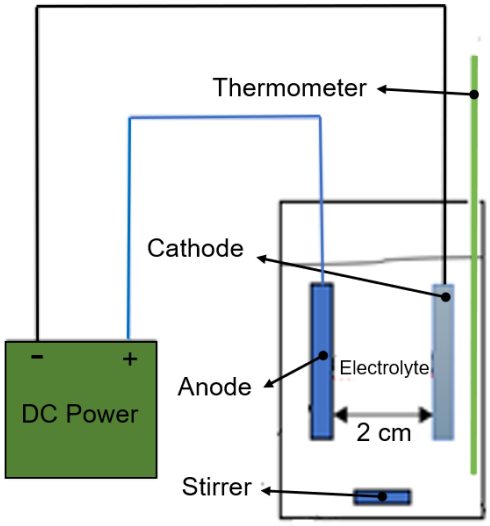

Figure 1. Electroplating process [17]..

Electroplating requires careful control of several parameters to achieve the desired coating quality. The primary parameters influencing the process include current density, electrolyte pH, and deposition time. In addition to these, other factors such as the addition of surfactants, particle concentration, and particle type can also affect the coating performance [18]. In general, the coating thickness increases proportionally with deposition time and applied current. According to Faraday's law, the total electric charge (Q) in the electrolyte is directly proportional to the current (I) and the time (t) [19].

This study aims to investigate the effect of current density on the surface morphology of Ni coatings deposited on Zr-2 using the electroplating method.

 DOI: https://doi.org/10.55981/urania.2025.9199

METHODOLOGY

For the preparation of the Ni electrolyte solution, the following chemicals were used: 200 g/L $NiSO_4 \cdot 6H_2O$ as the nickel source, 35 g/L $NiCl_2 \cdot 6H_2O$ as the activator, and 30 g/L H_3BO_3 as the pH buffer. The composition of the electrolyte solution and the parameters applied during the electroplating process are summarized in Table 1.

This study using three samples with different current densities: sample 1 at 0.015 A/cm², sample 2 at 0.025 A/cm², and sample 3 at 0.05 A/cm². The deposition time during the electroplating process was determined using Faraday's law, as expressed in equations (1), (2), and (3), under the assumption of a uniform surface formation [20]. Based on these equations, the calculated deposition times required to obtain a 6 µm Ni layer on a Zr-2 substrate with a surface area of 2 cm² were 19 minutes for sample 1, 11 minutes for sample 2, and 6 minutes for sample 3.

$$W = \frac{I \times t \times e}{96500} \quad (1)$$

$$\text{Density} = \frac{\text{Deposit weight (gram)}}{\text{Volume (cm}^3\text{)}} \quad (2)$$

$$\text{Thickness} = \frac{\text{Volume (cm}^3\text{)}}{\text{Surface Area (cm}^2\text{)}} \quad (3)$$

With W as the deposit weight (g), I as the current (A), t as the deposition time (s), and e as the electrochemical equivalent (M.A/valence).

Table 1. Composition of the electrolyte solution and process parameters.

Component	Concentration (g/L)	Function
$NiSO_4.6H_2O$	200	Nickel source
$NiCl_2.6H_2O$	35	Activator
H_3BO_3	30	Buffer
Plating Conditions		
pH	4	
Temperature	<25°C	
Anode	Platina	
Zr-2 surface area	2 cm²	
Current densities	0.015 A/cm²; 0.025 A/cm²; and 0.05 A/cm²	

Surface morphology was characterized using a Phenom-Pharos Desktop Scanning Electron Microscope (SEM), while microhardness measurements were performed using the Vickers method at the Testing Laboratory of Radiometallurgy Installation – Nuclear Fuel Installation (IRM-IBBN), Tangerang Selatan.

RESULT AND DISCUSSION

The deposition of Ni on the Zr-2 surface via the electroplating method was examined using SEM. The SEM images were further processed using ImageJ software to quantify the pore area (highlighted in yellow), as shown in Figure 2. The analysis revealed pore areas of 6.5 µm² for Sample 1, 20.85 µm² for Sample 2, and 27.98 µm² for Sample 3. It was observed that increasing current density resulted in larger pore areas.

From the SEM results shown in Figure 2, the nickel coating forms irregular nodular structures on the surface. A total of 25 nodules were randomly selected for measurement, and their average diameters were calculated using ImageJ software. The results of the ImageJ analysis are summarized in Table 2. The average nodule diameter for Sample 1 was 4.68 µm, for Sample 2 was 6.19 µm, and for Sample 3 was 6.84 µm. The nodule size was found to increase proportionally with current density, indicating that higher current densities promote the formation of larger nickel nodules.

Meanwhile, the surface composition was analyzed using Energy Dispersive X-ray Spectroscopy (EDS), and the results are presented in Figure 3. All three samples exhibited similar EDS spectra, indicating a homogeneous distribution of Ni across the Zr-2 substrate surface.

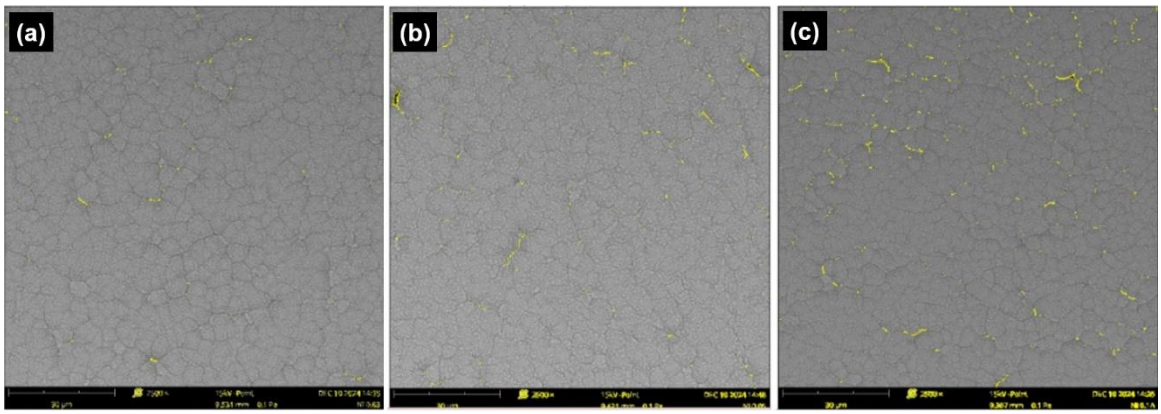

Figure 2. SEM image analysis using ImageJ, (a) Sample 1; (b) Sample 2; and (c) Sample 3.

Table 2. Average diameter of Ni nodules obtained from ImageJ analysis.

Sample 1 (µm)	Sample 2 (µm)	Sample 3 (µm)
6.67	6.23	4.66
5.02	4.79	7.32
6.68	6.51	7.84
5.11	6.79	5.53
4.31	6.06	9.79
3.69	5.27	6.72
3.43	7.56	4.44
5.09	5.15	6.36
4.81	4.06	7.87
5.41	6.15	6.90
4.97	5.54	6.18
3.69	5.17	6.52
3.68	7.54	7.44
4.33	4.49	10.61
5.08	5.51	6.49
4.96	7.33	7.34
3.82	7.17	7.46
4.65	6.05	5.53
1.82	7.02	5.73
4.53	4.93	6.98
3.53	7.35	6.45
5.92	7.77	7.23
6.90	5.40	6.87
4.13	7.75	6.57
4.69	7.22	6.11
4.68	6.19	6.84

Meanwhile, the surface composition was analyzed using Energy Dispersive X-ray Spectroscopy (EDS), and the results are presented in Figure 3. All three samples exhibited similar EDS spectra, indicating a homogeneous distribution of Ni across the Zr-2 substrate surface.

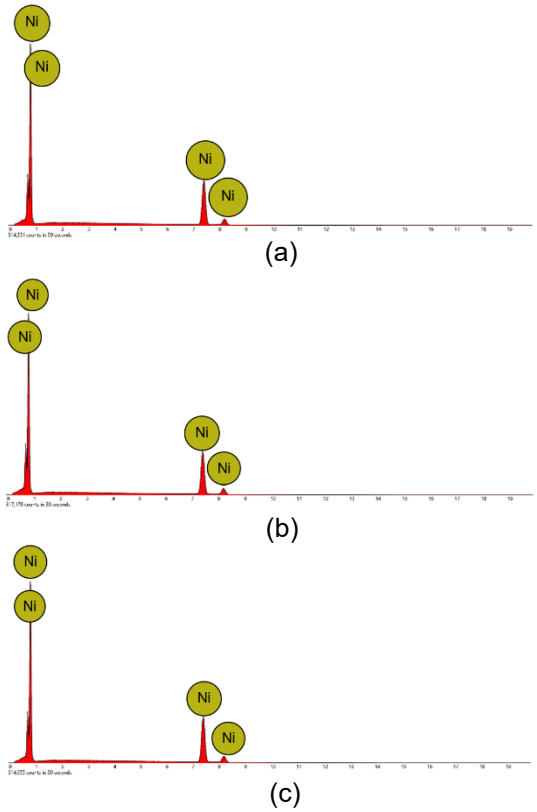

Figure 3. EDS results: (a) Sample 1; (b) Sample 2; and (c) Sample 3.

To evaluate the effect of current density on surface hardness, micro-Vickers hardness testing was conducted, and the results are presented in Figure 4 and Table 3. The results indicate that current density significantly influences surface hardness; as the applied current density during the electroplating process increases, the hardness values also increase.

 DOI: https://doi.org/10.55981/urania.2025.9199

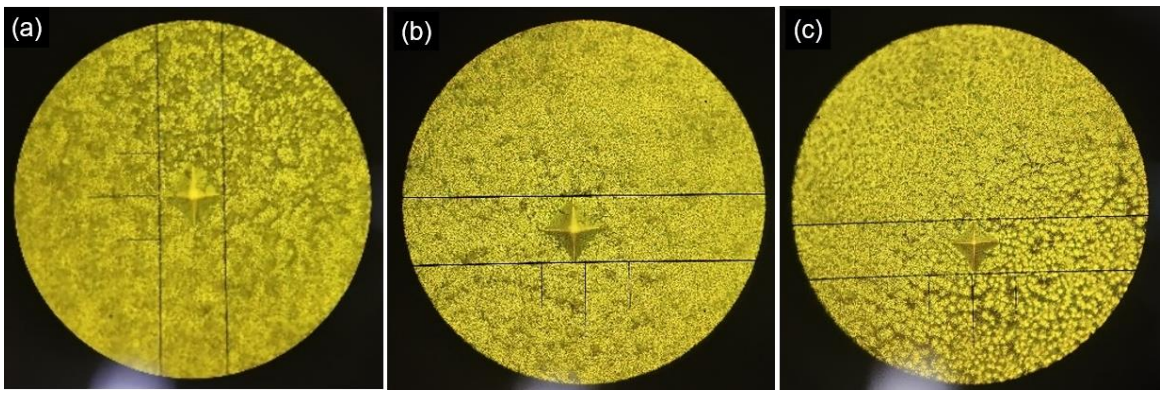

. Figure 4. Micro-Vickers hardness test results, (a) Sample 1; (b) Sample 2; and (c) Sample 3

Table 3. Micro-Vickers hardness test results.

Sample	D1 (μm)	D2 (μm)	Average HV
Sample 1	42.46	48.11	163.48
	43.79	46.88	
	45.19	51.27	
	47.76	48.40	
Sample 2	41.87	44.87	178.35
	43.53	45.98	
	44.34	45.32	
	44.77	46.97	
Sample 3	35.83	36.10	234.25
	38.07	40.75	
	40.80	38.83	
	41.59	41.18	

After the surface morphology observations, cross-sectional analysis was conducted to determine the coating thickness using SEM at a magnification of 2500×, as shown in Figure 5. The cross-sectional results revealed that Sample 1 exhibited no defects in the coating layer, whereas Samples 2 and 3 showed defects at the Ni–Zr-2 interface, indicated by the arrows in Figure 5. In addition to these defects, thin gaps between the coating and substrate were also observed in Samples 2 and 3, while Sample 1 showed no visible gaps.

The coating thickness was further measured using ImageJ. The thickness of Sample 1 was 7.44 μm, Sample 2 was 19.17 μm, and Sample 3 was 8.42 μm. The variation in thickness values, which did not correspond well with the theoretical calculations, may be attributed to several factors, including the non-uniform distance between the anode and cathode and the reduction in electrolyte concentration, which could affect the ion deposition rate.

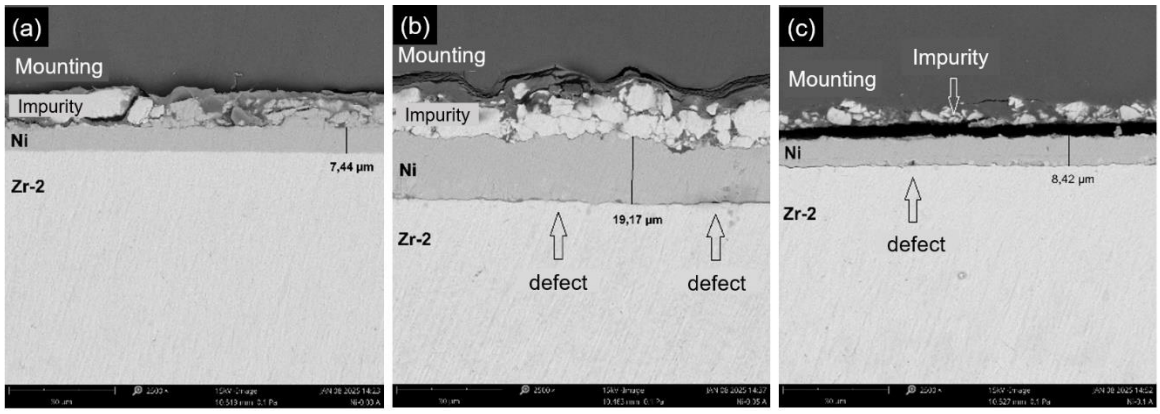

Figure 5. Cross-sectional SEM images: (a) Sample 1; (b) Sample 2; and (c) Sample 3.

The defect observed in Figure 5(b) was further analyzed using EDS, which revealed the presence of trapped oxygen and carbon, as shown in Figure 6. The presence of oxygen at the coating–substrate interface likely occurred during the electroplating process, leading to reduced adhesion between the substrate and the Ni layer.

Additionally, oxygen at the interface contributed to the appearance of carbon contamination during polishing with SiC paper.

The impurities observed in the cross-sectional SEM of Figure 5 are therefore attributed to sample preparation prior to SEM analysis. This interpretation is supported by the comparison with the surface EDS results in Figure 3, where the Ni layer was found to be uniformly distributed, in contrast to the localized impurities detected in the cross-section.

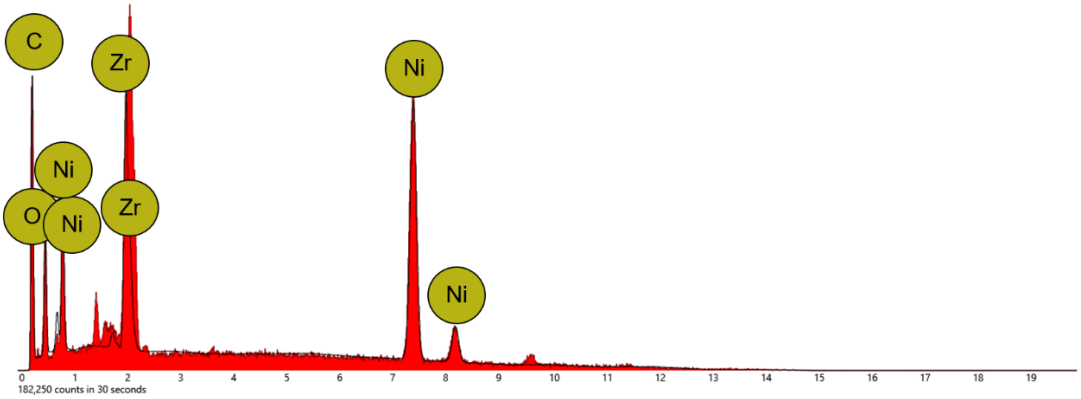

Figure 6. EDS analysis of Sample 2

As shown in Figure 7, the EDS line-scan analysis confirmed the presence of Ni, C, and Zr. The green region corresponds to the Zr-2 substrate, which is highly dominant on the right side. The yellow region represents Ni, which is strongly concentrated in the middle, corresponding to the coating area. The detection of Ni and Zr-2 signals outside the coating region is attributed to the polishing process of the samples. The blue region indicates a high concentration of carbon on the outermost surface of the coating, which originated from contamination and the use of SiC during polishing. In addition, the oxygen layer observed in Figure 7(b) is likely the result of electroplating reactions or subsequent oxidation of the sample by the environment.

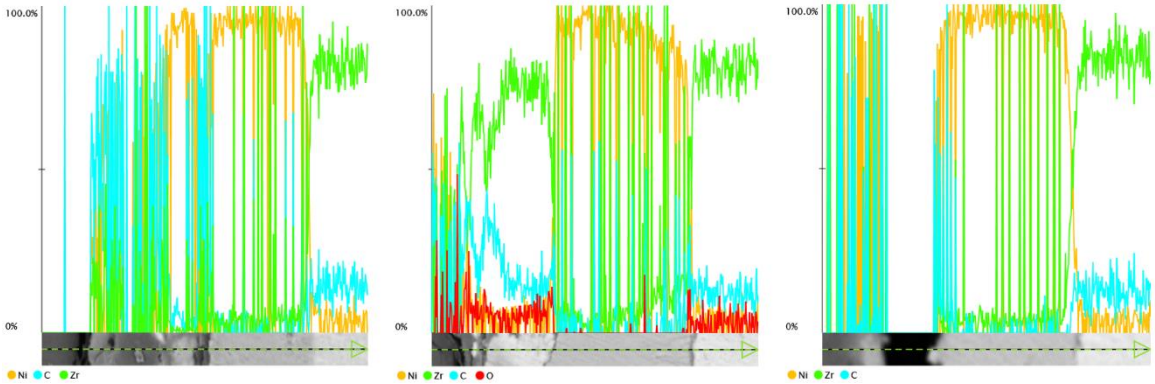

(a) (b) (c)

Figure 7. EDS line-scan results: (a) Sample 1; (b) Sample 2; and (c) Sample 3.

CONCLUSION

An increase in current density leads to larger nickel grain size and higher pore area on the coating surface. Higher current density also enhances the surface hardness of the nickel layer. However, cross-sectional SEM analysis revealed that a current density of 0.015 A/cm² provides superior coating quality compared to higher current densities, as defects and interfacial gaps were observed at 0.025 and 0.05 A/cm². To minimize surface contamination, ultrasonic cleaning should be performed prior to SEM characterization.

 DOI: https://doi.org/10.55981/urania.2025.9199

ACKNOWLEDGEMENTS

The authors would like to express their gratitude to the BRIN Research-Based Graduate Program for funding the Master's study in Materials Science at Universitas Indonesia. Special thanks are also extended to my laboratory colleagues for their support of this research.

REFERENCES

[1] J. C. Brachet *et al.*, "High temperature steam oxidation of chromium-coated zirconium-based alloys: Kinetics and process," *Corros Sci*, vol. 167, p. 108537, May 2020, doi: 10.1016/J.CORSCI.2020.108537.

[2] J. C. Brachet *et al.*, "Early studies on Cr-Coated Zircaloy-4 as enhanced accident tolerant nuclear fuel claddings for light water reactors," *Journal of Nuclear Materials*, vol. 517, pp. 268–285, Apr. 2019, doi: 10.1016/J.JNUCMAT.2019.02.018.

[3] S. Yeo, J. H. Kim, and H. S. Yun, "Effect of pulse current and coating thickness on the microstructure and FCCI resistance of electroplated chromium on HT9 steel cladding," *Surf Coat Technol*, vol. 389, p. 125652, May 2020, doi: 10.1016/J.SURFCOAT.2020.125652.

[4] J. Yang *et al.*, "Review on chromium coated zirconium alloy accident tolerant fuel cladding," *J Alloys Compd*, vol. 895, p. 162450, Feb. 2022, doi: 10.1016/J.JALLCOM.2021.162450.

[5] D. V. Sidelev, C. Poltronieri, M. Bestetti, M. G. Krinitcyn, V. A. Grudinin, and E. B. Kashkarov, "A comparative study on high-temperature air oxidation of Cr-coated E110 zirconium alloy deposited by magnetron sputtering and electroplating," *Surf Coat Technol*, vol. 433, p. 128134, Mar. 2022, doi: 10.1016/J.SURFCOAT.2022.128134.

[6] N. Capps and R. Sweet, "Model for determining rupture area in Zircaloy cladding under LOCA conditions," *Nuclear Engineering and Design*, vol. 401, Jan. 2023, doi: 10.1016/J.NUCENGDES.2022.112096.

[7] P. Baque, R. Darras, A. Lafon, and H. Loriers, "Protection du zirconium contre l'oxydation au moyen de revetements metalliques," *Journal of Nuclear Materials*, vol. 25, no. 2, pp. 166–171, Feb. 1968, doi: 10.1016/0022-3115(68)90042-1.

[8] Z. Yang, Y. Niu, J. Xue, T. Liu, C. Chang, and X. Zheng, "Steam oxidation resistance of plasma sprayed chromium-containing coatings at 1200 °C," *Materials and Corrosion*, vol. 70, no. 1, pp. 37–47, Jan. 2019, doi: 10.1002/maco.201810156.

[9] W. G. Luscher, E. R. Gilbert, S. G. Pitman, and E. F. Love, "Surface modification of Zircaloy-4 substrates with nickel zirconium intermetallics," *Journal of Nuclear Materials*, vol. 433, no. 1–3, pp. 514–522, 2013, doi: 10.1016/j.jnucmat.2012.05.039.

[10] M. Huang, Y. Li, G. Ran, Z. Yang, and P. Wang, "Cr-coated Zr-4 alloy prepared by electroplating and its in situ He+ irradiation behavior," *Journal of Nuclear Materials*, vol. 538, p. 152240, Sep. 2020, doi: 10.1016/J.JNUCMAT.2020.152240.

[11] H. Okamoto, "Ni-Zr (nickel-zirconium)," *J Phase Equilibria Diffus*, vol. 28, no. 4, p. 409, Aug. 2007, doi: 10.1007/S11669-007-9120-Z/FIGURES/1.

[12] D. V. Sidelev, E. B. Kashkarov, M. S. Syrtanov, and V. P. Krivobokov, "Nickel-chromium (Ni–Cr) coatings deposited by magnetron sputtering for accident tolerant nuclear fuel claddings," *Surf Coat Technol*, vol. 369, pp. 69–78, Jul. 2019, doi: 10.1016/J.SURFCOAT.2019.04.057.

[13] S. Shankar, D. E. Koenig, and L. E. Dardi, "Vacuum Plasma Sprayed Metallic Coatings," *JOM: Journal of The Minerals, Metals & Materials Society*, vol. 33, no. 10, pp. 13–20, Dec. 1981, doi: 10.1007/BF03339507/METRICS.

[14] V. Kuzmin, I. Gulyaev, D. Sergachev, S. Vaschenko, E. Kornienko, and A. Tokarev, "Equipment and technologies of air-plasma spraying of functional coatings," *MATEC Web of Conferences*, vol. 129, p. 01052, Nov. 2017, doi: 10.1051/MATECCONF/201712901052.

[15] R. Vilar, "Laser cladding," *J Laser Appl*, vol. 11, no. 2, pp. 64–79, Apr. 1999, doi: 10.2351/1.521888.

[16] V. Boronenkov and Y. Korobov, "Fundamentals of arc spraying: Physical and chemical regularities," *Fundamentals of Arc Spraying: Physical and Chemical Regularities*, pp. 1–256, Jan. 2016, doi: 10.1007/978-3-319-22306-3/COVER.

[17] C. qun LI, X. hai LI, Z. xin WANG, and H. jun GUO, "Nickel electrodeposition from novel citrate bath," *Transactions of Nonferrous Metals Society of China*, vol. 17, no. 6, pp. 1300–1306, Dec. 2007, doi: 10.1016/S1003-6326(07)60266-0.

[18] E. S. Güler, "*Effects of Electroplating Characteristics on the Coating Properties*," Electrodeposition *of Composite Materials*, Mar. 2016, doi: 10.5772/61745.

[19] D. Topayung, "Pengaruh Arus Listrik dan Waktu Proses Terhadap Ketebalan dan Massa Lapisan yang Terbentuk pada Proses Elektroplating Pelat Baja," *Jurnal Ilmiah Sains*, vol. 11, no. 1, pp. 97–101, Apr. 2011, doi: 10.35799/JIS.11.1.2011.50.

[20] A. Rasyad *et al.*, "Analisis Pengaruh Temperatur, Waktu, dan Kuat arus Proses Elektroplating Terhadap Kuat Tarik, Kuat Tekuk dan Kekerasan pada Baja Karbon Rendah," *Jurnal Rekayasa Mesin*, vol. 9, no. 3, pp. 173–182, 2018.

 DOI: https://doi.org/10.55981/urania.2025.9199